# Photo-acoustic A-scanning and monitoring of blood content in tissue

Roy G.M. Kolkman*, Magdalena C. Pilatou, Erwin Hondebrink, Frits F. M. De Mul

University of Twente, Department of Applied Physics,
POBox 217, 7500 AE Enschede, the Netherlands

## ABSTRACT

To localize and monitor the blood content in tissue we developed a very sensitive double-ring photo-acoustical detector. PVdF has been used as piezo-electric material. In this detector also a fiber for illumination of the sample is integrated. This detector has the advantage that it is very sensitive in the forward direction. A ratio of FWHM to depth of 1:70 can be obtained with this detector.

**Keywords:** Photoacoustics, piezoelectric transducer, tissue, blood

## 1. INTRODUCTION

In recent years a broad interest exists in developing new techniques for non-invasively monitoring structures in tissue. The purpose is to replace X-ray and other oppressing techniques. Various techniques are based on light scattering in tissue. In highly scattering media, like dermal tissue, the scattering coefficient not only determines the penetration depth, but also the resolution which can be achieved by the technique. With photoacoustic (PA) signal generation (figure 1), the amplitude depends on the local fluence-rate only. The preceding light path of the photon, caused by scattering is not relevant. PA can be performed in pulsed mode or modulation mode. The first gives the highest PA signal amplitudes.

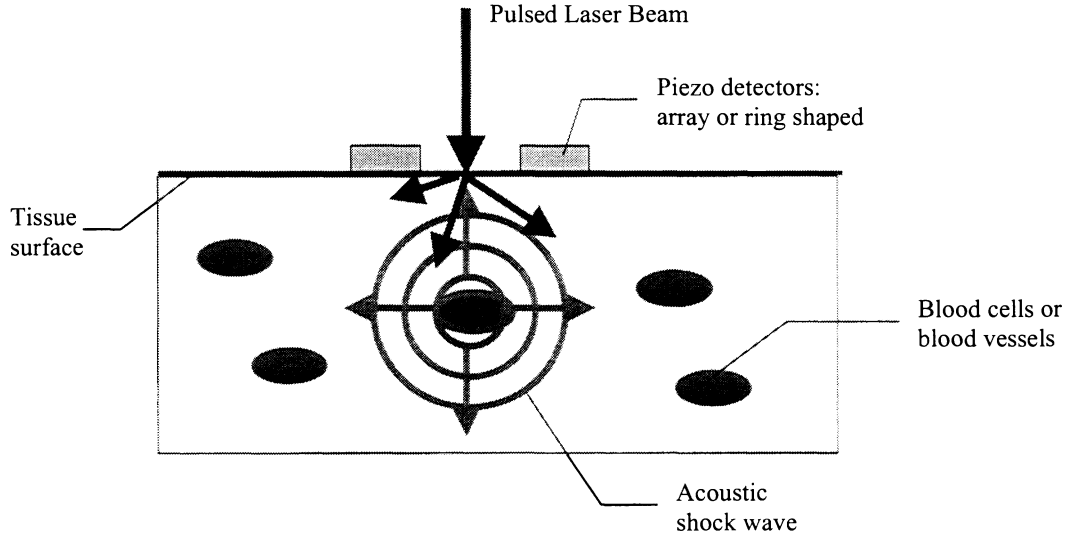


**Figure 1:** Photoacoustic signal generation. A laser light pulse is absorbed by the blood. The absorption causes an adiabatic temperature rise and pressure build up which results in an acoustic shock wave. This wave propagates to the tissue surface where it can be detected by small pressure transducers.

* Correspondence: Email: R.G.M.Kolkman@tn.utwente.nl; Telephone ++31 53 489 3870; Fax ++31 53 489 1105



In *Biomedical Optoacoustics*, Alexander A. Oraevsky, Editor,
Proceedings of SPIE Vol. 3916 (2000) • 1605-7422/00/$15.00

By measuring the pressure as a function of time and position in the detection plane, a PA image can be reconstructed. It is shown that photoacoustics is a promising technique to visualize absorbing structures in tissue like media[1-6]. The depth resolution we can obtain is 10 μm, with a spatial resolution of 200 μm[1,3,5,6]. These measurements have been performed using small (200 μm diameter) piezo detectors. These detectors have a very large opening angle, which is used in the image algorithm to obtain the lateral resolution. The maximum reachable depth is limited to about 10 mm at a wavelength of 550 nm due to scattering and absorption in the surrounding tissue. As the scattering decreases with the wavelength, the wavelength should be shifted to about 850 nm to reach a larger depth. The sensitivity then will be less due to the decreased absorption contrast. In table 1 some characteristic properties of tissue and blood are summarized.

**Table 1.** Typical optical properties of blood and tissue at relevant wavelengths.

| | *Reduced scattering coefficient:* $\mu_s'$ *[mm$^{-1}$]* | | *Absorption coefficient:* $\mu_a$ *[mm$^{-1}$]* | |
|---|---|---|---|---|
| | λ = 580 nm | λ = 850 nm | λ = 580 nm | λ = 850 nm |
| Dermis | 3 | 1 | 0.03 | 0.01 |
| Blood | 1 | 0.5 | 32 | 1.2 |

In stead of a small disk detector also a ring detector can be used. The latter one has a very small opening angle, compared to the disk detector. This gives the ability to make a-scans of the tissue or to monitor the blood content on a line in depth. An application for this detector is localizing and monitoring the blood content in the neonates brain. For this purpose a detector is needed which is very sensitive and which has a small opening angle. To reach a large depth, near infrared (850 nm) light should be used in stead of green (580 nm) light.

## 2. METHOD

The response of a ring detector to a spherical Gaussian heat source (radius $R_\sigma$) can be calculated[7]. The source is illuminated by a laser pulse with a duration of $2\tau_l$ of which a total amount of energy $E_a$ is absorbed. This source is surrounded by a medium with a thermal expansion coefficient β, specific heat capacity $c_p$ and longitudinal acoustic phase velocity v. The pressure P (r,t) at a distance r from the spherical Gaussian source at time t can be described by[7]

$$P(r,t) = -P_{\max}(r)\sqrt{e}\,\frac{t-\tau}{\tau_e}\exp\left\{-\frac{1}{2}\left(\frac{t-\tau}{\tau_e}\right)^2\right\}$$

$$P_{\max}(r) = \frac{\beta E_a}{2\sqrt{e}(2\pi)^{3/2} c_p \tau_e^{\,2} r} \qquad (1)$$

$$\tau = \frac{r}{v}; \qquad \tau_e = \sqrt{\tau_a^{\,2} + \tau_l^{\,2}}; \qquad \tau_a = \frac{R_\sigma}{v}.$$

To obtain the response of the detector, the output voltage $V_p$ of the detector has to be calculated. For thin film piezoelectric sensors only the thickness mode is relevant. If the thickness of the piezo is much smaller than the wavelength, the piezoelectric voltage can be expressed as

$$V_p(\mathbf{r},t) = g_{33}\frac{d\int_A P(\mathbf{r},t)T_A(\mathbf{r})\cos(\theta_2(\mathbf{r}))dA}{A} \qquad (2)$$

$$T_A = \frac{2Z_2'}{Z_2'+Z_1'}; \quad Z_1' = \frac{\rho_1 v_1}{\cos\theta_i}; \quad Z_2' = \frac{\rho_2 v_2}{\cos\theta_2}$$

$T_A(\mathbf{r})\cos(\theta_2(\mathbf{r}))$ represents the normal component of the transmitted pressure amplitude from liquid to the piezo electrical material[8]. $\rho_1$, $\rho_2$ represent the density of the liquid respectively solid. $\theta_i$, $\theta_2$ represents the angle with the normal of the incident wave and transmitted wave respectively. In these calculations the absorption of sound is not taken into account.
The detector can be characterized by calculating the depth sensitivity and directional sensitivity. The depth sensitivity of the ring detector is calculated for a point source on the midline (x = 0) of the detector as a function of depth z (figure 2). The directional sensitivity is defined as the response of the detector to a source at a certain depth z as a function of x. The source is assumed to generate an acoustic wave with a peak to peak time of 12 ns (83 MHz).

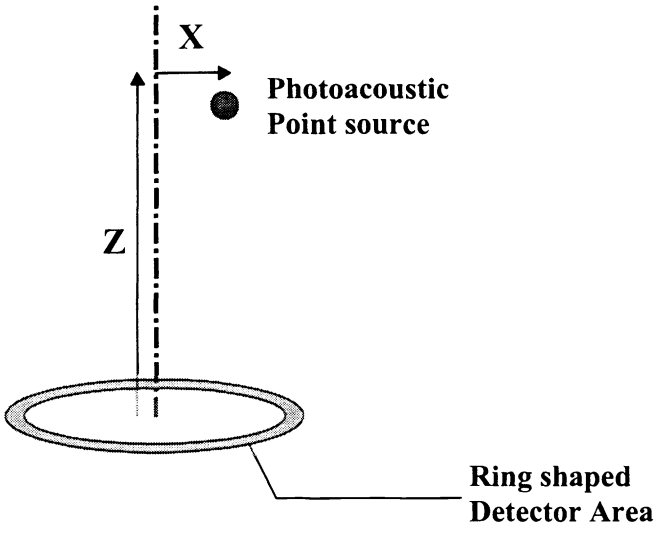


**Figure 2:** Geometry used to calculate depth sensitivity and directional sensitivity of a ring detector. The dimensions of the ring are defined by the inner radius $R_i$ and the outer radius $R_o$.

The directional sensitivity has been calculated for various ring dimensions. In figure 3 the directional sensitivity at a depth of 10 mm is shown for an inner radius of 2.0 mm and 3 different outer radii: 2.1, 2.3, and 2.5 mm.

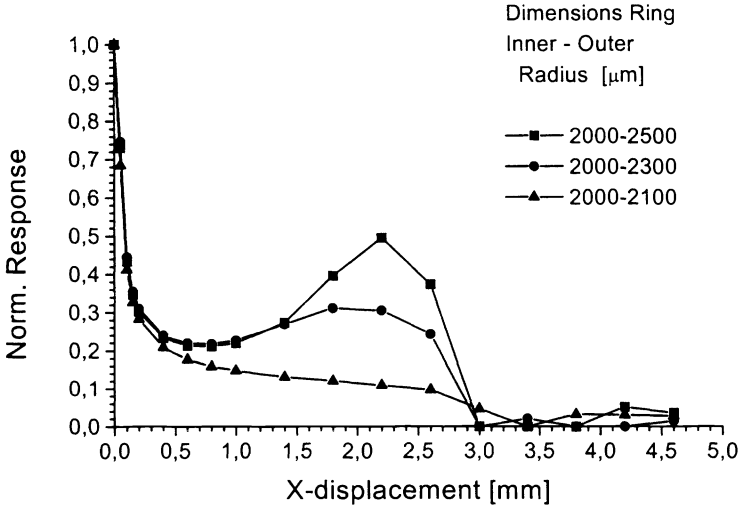


**Figure 3:** Directional response of ring detector for a point source at a depth z of 10 mm.

Figure 3 shows that with increasing outer radius of the ring, a side-lobe in the directional response of the detector appears. This side lobe is located in front of the ring surface. As this is unwanted the outer radius of the ring should be as small as possible. Another opportunity to suppress these side-lobes is using two concentric rings as electrodes with different dimensions. The side lobes then appear at different distances from the midline of the rings, which can be used by signal processing to suppress these side-lobes.
Another important parameter is the HWHM (half width half maximum) of the directional response curve. For various ring dimensions and depths these values are plotted in figure 4.

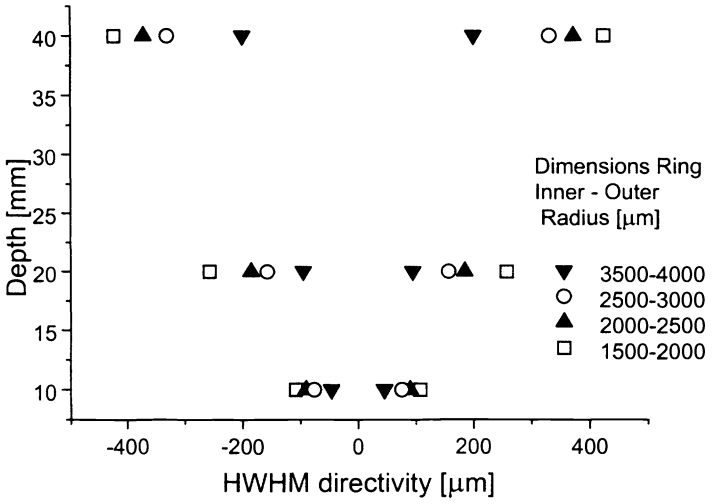


**Figure 4:** HWHM of directional response curves for various ring dimensions and depths.

Figure 4 shows that for example a ring detector with an inner radius of 3.5 and an outer radius of 4.0 mm gives a ratio of FWHM to depth of about 1 to 100.
The depth sensitivity of a ring detector is plotted in figure 5 for 3 different ring dimensions.

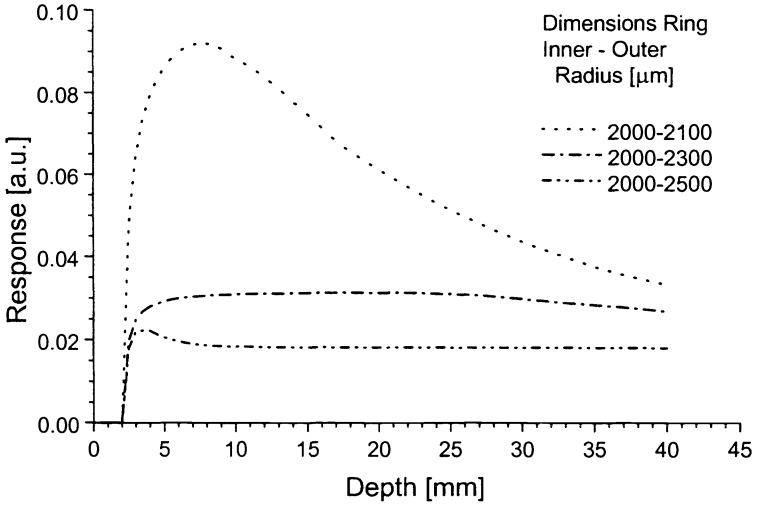


**Figure 5:** Depth sensitivity of a PA ring detector as a function of the ring dimensions.

From figure 5 it appears that the larger the ring area, the more destructive interference occurs of the PA signals at the ring surface.
Based on these calculated detector characteristics and some practical considerations, a double ring detector has been constructed consisting of two concentric rings:

- Inner ring: $R_i = 2.0$ mm, $R_o = 2.3$ mm
- Outer ring: $R_i = 3.5$ mm, $R_o = 3.8$ mm

Figure 6 shows a schematic representation of this detector. At the midline of this detector a 600 μm core diameter glass fiber is placed to deliver the light to the tissue. As piezoelectric material 9 μm thick, polyvinylidene difluoirde (PVdF) is used. The top layer of this PVdF consists of a 50 nm gold layer which is grounded. In this detector an amplifier is integrated with a total amplification of 58 dB. The housing is made of brass to electrically shield the electronics.

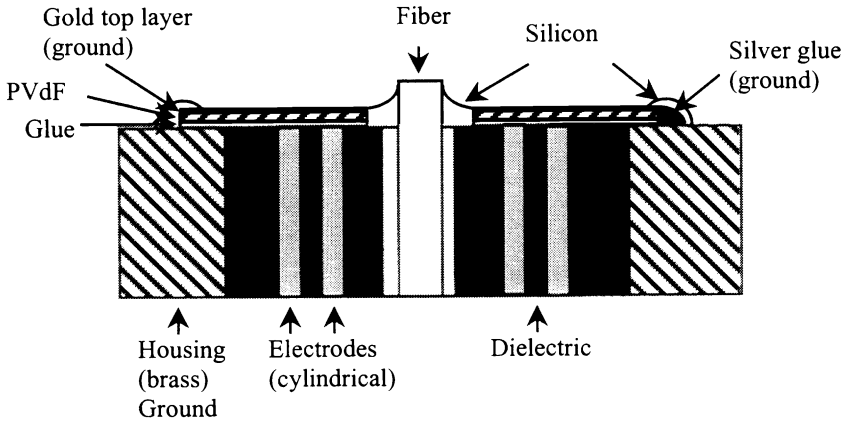


**Figure 6:** Schematic cross-section of detector; detector is cylindrical symmetrical; dimensions not on scale

To perform the PA measurements a Nd:YAG laser, frequency doubled (532nm) with 15 ns pulses and a repetition rate of 50 Hz (LS 2139, Lotis TII) is used. The signals are collected and averaged by a 1 Gsample/s, two channel digital oscilloscope (TDS-220, Tektronix) and transferred to the computer for further processing. (figure 7)

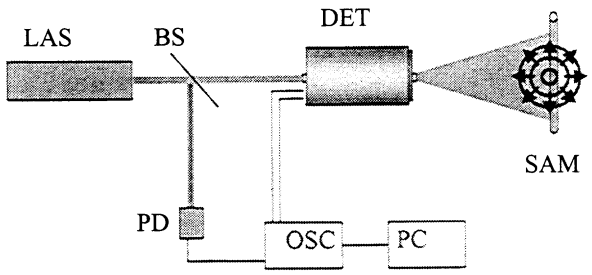


**Figure 7:** Schematic representation of measurement setup. LAS: Nd:YAG laser; BS: Beam splitter; PD: Photodiode (triggering); OSC: Oscilloscope; PC: Personal computer; DET: Detector; SAM: Sample.

The signals of both rings are separately read out by the computer. A Labview programm (National Instruments) then corrects for the time difference in arrival of the signal at the two rings (figure 8).

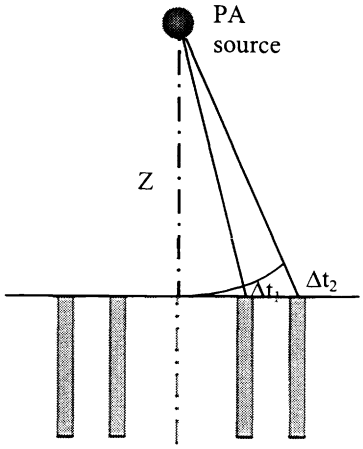


**Figure 8:** Time difference in arrival of signals at inner ($\Delta t_1$) and outer ($\Delta t_2$) ring. The electrodes of the inner and outer ring are depicted in gray.

## 3. RESULTS AND DISCUSSION

Testing the detector has been carried out using a 200 μm diameter black hair placed in water as a sample. In figure 9 the signals of both rings are shown separately before correction for the time delay.

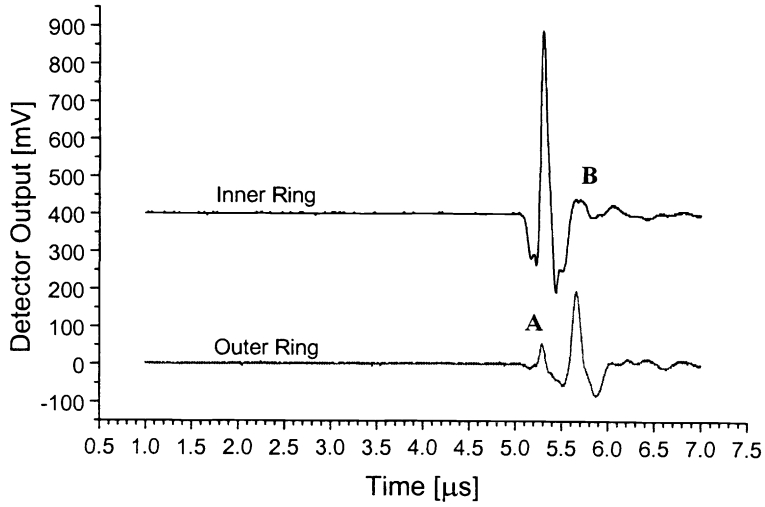


**Figure 9:** Signals from inner and outer ring; not corrected for the time delay. The signal of the inner ring is shifted over 400 mV. Sample: black hair in water; 128 averages.

The signal of the inner ring is 2.5 times larger than the signal of the outer ring. A part of this is caused by more destructive interference of the PA signals at the (larger) outer ring surface. This results, according to the calculations in a 1.5 times lower signal at a depth of 8 mm. The other factor 1.7 is caused by a difference in amplification of the electronics used to amplify the signals. From figure 9 can also be seen that there is a electronic coupling between the two amplifier circuits. In

the signal of the outer ring a small peak (A) appears when the inner ring detects a signal. This also holds for the inner ring; there the peak (B) is smaller.
After correction for the time-delay in arrival between the inner and outer ring, the signals can be further processed. One way to calculate the final signal is adding up the signals of both rings. In this case the relative contribution of the peaks caused by the electronic coupling is decreased, but still present. Another way of calculating the final signal is multiplying both signals and after that recalculation of the signal-shape. This has the advantage that the peaks which are caused by the electronic coupling almost completely disappear: these peaks are artifacts and thus not present in the signal of the other ring. The result of the two different ways of signal processing is shown in figure 10.

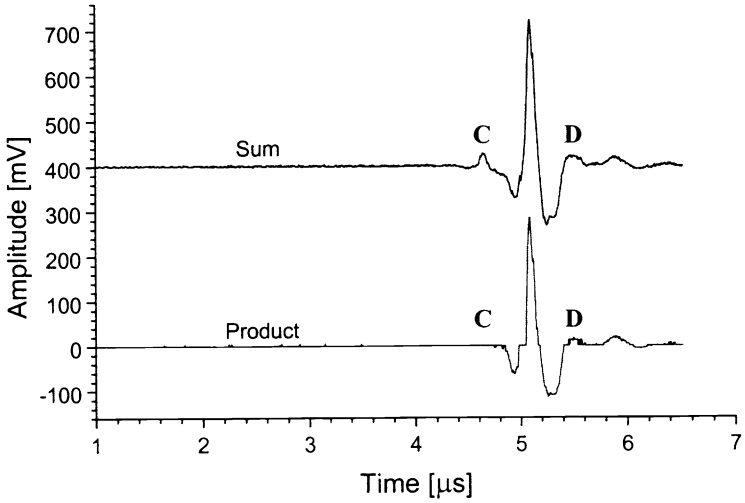


**Figure 10:** Two different ways of calculating the final signal: summing the ring data and calculating the product and retrieving back the original signal shape. The sum-signal is shifted over 400 mV.

From figure 10 can be seen that the small positive peak (C) (due to electronic coupling of the outer ring with the inner ring electronics) before the large peak is completely disappeared in the signal calculated by multiplying the signals. The other peak (D) is decreased by calculating the product.

## 4. CONCLUSIONS

With this photoacoustic ring detector it is possible to make a-scans of tissue structures. The detector has a ratio of FWHM : Depth of 1 : 70. This means that it only detects photoacoustic sources which are located at the midline of the detector. An application of this detector will be monitoring of the blood content in the neonates brain. For this purpose PA sources (eg. Blood) have to be detected up to a depth of about 4 cm. This implies that near infrared light (~850 nm) has to be used in stead of green (~550 nm) light.

## 5. ACKNOWLEDGEMENT

This research was sponsored by the Dutch Technology Foundation STW (Grant TTN.4661).

## REFERENCES


1. C.G.A. Hoelen, R.G.M. Kolkman, M. Letteboer, R. Berendsen and F.F.M. de Mul, "Photoacoustic Tissue Scanning (PATS)", *Optical Tomography and Spectroscopy of Tissue III*, SPIE Vol. **3597**, pp. 336-343, 1999.
2. A.A. Oraevsky, V.A. Andreev, A.A. Karabutov, D.R. Fleming, Z. Gatalica, H. Singh and R.O. Esenaliev, "Laser Opto-Acoustic Imaging of the Breast: Detection of Cancer Angiogenisis", *Optical Tomography and Spectroscopy of Tissue III*, SPIE Vol. **3597**, pp. 352-363, 1999.
3. R.G.M. Kolkman, C.G.A. Hoelen, M.M.J. Letteboer, R.C.M. Berendsen and F.F.M. de Mul, "Photoacoustic Mapping of Hidden Tissue Structures", CLEO-Europe 99 (OSA), *Advances in Optical Imagin, Photon Migration, and Tissue Optics*, pp. 239-241, June 1999.
4. A.A. Oraevsky, "Opto-acoustic tomography of deeply embedded tumors and early subsurface lesions", CLEO-Europe 99 (OSA), *Advances in Optical Imagin, Photon Migration, and Tissue Optics*, pp. 236-238, June 1999.
5. C.G.A. Hoelen and F.F.M. de Mul, "Imaging of cutaneous blood vessels using photoacoustic tissue scanning (PATS)", SPIE-BIOS 98 conference Stockholm, *Photon Migration in Tissues*, chair D. Benaron et al., vol. **3566**, contr. Nr. 20, 1998.
6. C.G.A. Hoelen, F.F.M. de Mul, R. Pongers, A. Dekker, "Three dimensional photoacoustic imaging of blood vessels in tissue", Optics letters, **28**(3), April 1998.
7. C.G.A. Hoelen and F.F.M. de Mul, "A new theoretical approach to photoacoustic signal generation", J. Acoust. Soc. Am. **106**(2), pp. 695-706 , August 1999
8. V.M. Ristic, *Principles of Acoustic Devices*, Chapter 5: Piezoelectric bulk wave transducers, J. Wiley & Sons, New York, 1983.